

Glycine-Mediated Structural Evolution of ZnO Nanoparticles: A Robust Platform for Congo Red Mineralization and Glucose Detection

Jayasimha H N^{a*}, Chandrappa K G^{b*}, Dileepkumar V G^{a*}, Pruthviraj R D^c, Jobish Johns^c

^a Department of Chemistry, HKBK College of Engineering Bangalore – 560045 Karnataka, India

^b Department of Chemistry, Govt. Engineering College Ramanagar-562159 Karnataka, India

^c Department of Chemistry, Rajarajeswari College of Engineering, Bangalore, Karnataka, 560074, India

^d Department of Physics, Rajarajeswari College of Engineering, Bangalore, Karnataka, 560074, India

Corresponding Authors: Dr. Jayasimha H N – Jayasimha.sln@gmail.com

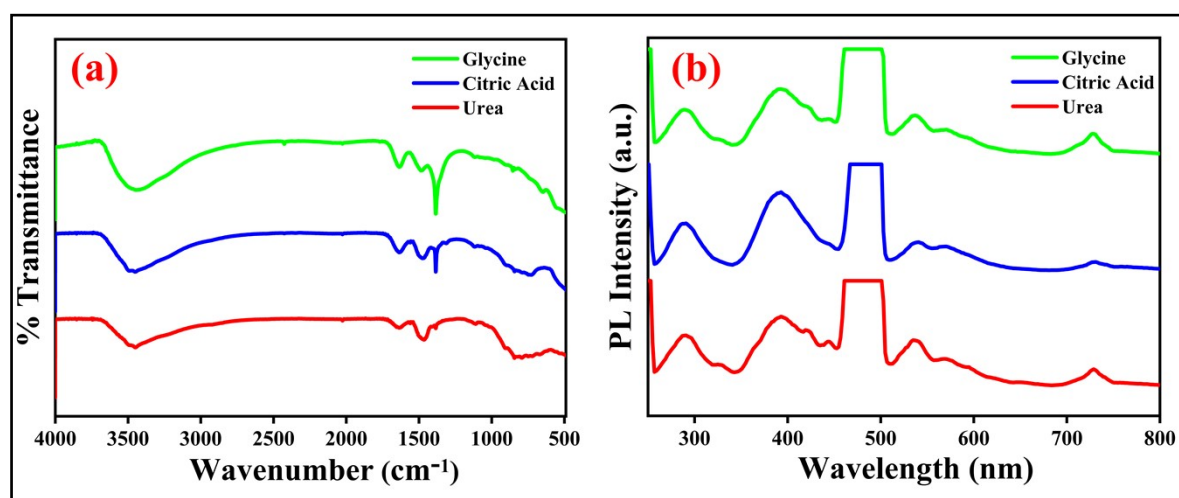
Dr. Chandrappa K G – Chandu.kodi@gmail.com

Dr. Dileepkumar V G – deepuvg29@gmail.com

Table S1: Pseudo first order rate constant values for the degradation of CR dye using glycine mediated ZnO nanoparticles.

Figure Number	Parameter	Rate constant	
S2. (a)	Comparison of different catalysts	ZnO-U	0.00735
		ZnO-CA	0.01137
		ZnO-G	0.01396
S2. (b)	Effect of catalyst dosage	10 mg	0.0052
		20 mg	0.00865
		30 mg	0.01396
		40 mg	0.01451
S2. (c)	Effect of initial dye concentration	10 ppm	0.01561
		20 ppm	0.01396
		30 ppm	0.00912
		40 ppm	0.00743
S2. (d)	Influence of radical scavengers	No scavengers	0.01396
		KI	0.00136
		CH ₃ OH	0.00294
		NaN ₃	0.00899
S2. (e)	Effect of solution pH	3	0.01396

		6	0.01002
		9	0.00601
		12	0.00398
S2. (f)	Reusability cycles	n=0	0.01396
		n=1	0.01303
		n=2	0.01157
		n=3	0.02779



Figure

re S1. (a) FTIR spectra of ZnO nanoparticles synthesized using glycine, citric acid and urea as fuels, showing the characteristic functional groups and Zn–O vibrational bands; (b) photoluminescence (PL) spectra of ZnO nanoparticles synthesized using different fuels, demonstrating their emission behavior and defect-related optical properties.

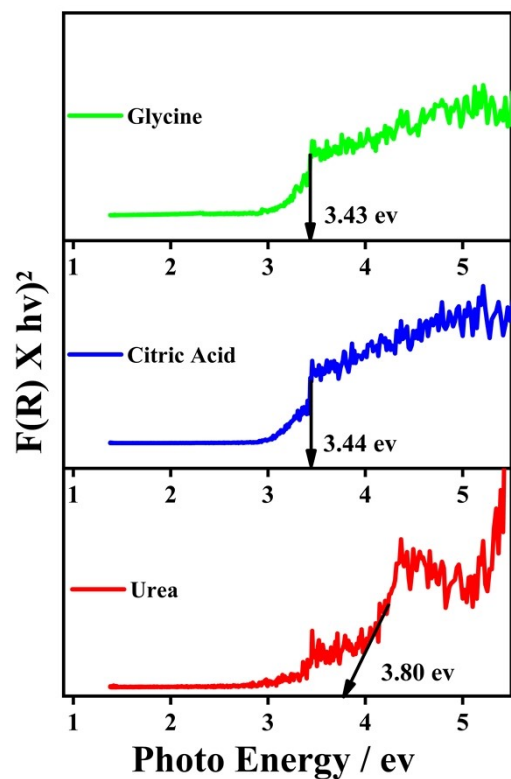


Figure S2: UV–DRS spectra and corresponding band gap energies of ZnO nanoparticles synthesized using glycine, citric acid and urea as fuels, showing optical absorption behavior and band gap values of 3.43, 3.44, and 3.80 eV, respectively.

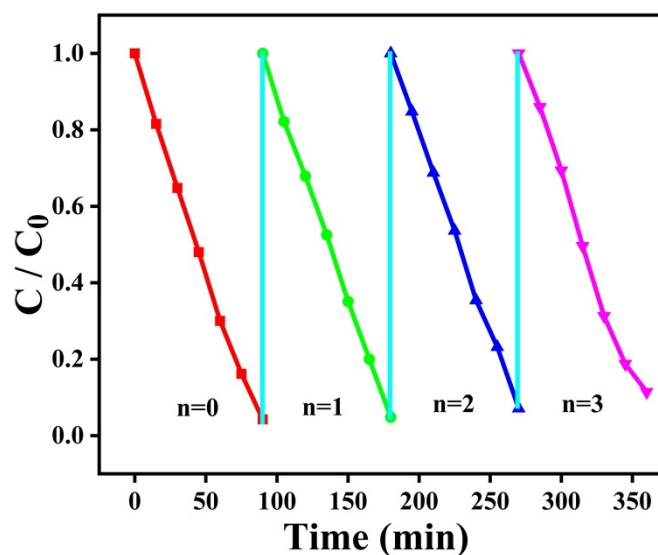


Figure S3. Recycling (reusability) test of the catalyst for photocatalytic degradation showing C/C_0 versus time over four consecutive runs ($n = 0-3$).

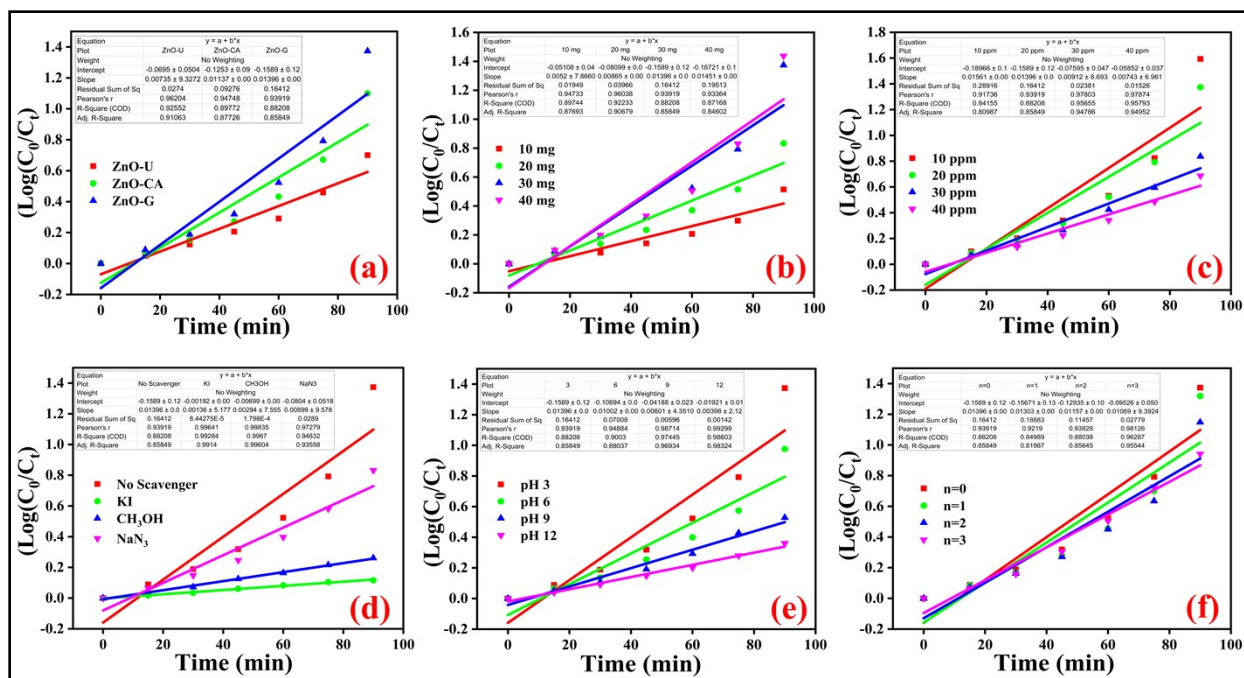


Figure S4. Pseudo-first-order kinetic plots for photocatalytic degradation, shown as $\ln(C_0/C_t)$ versus time under different conditions: (a) Comparison of different catalysts (ZnO-U, ZnO-CA, and ZnO-G), (b) effect of catalyst dosage (10–40 mg), (c) effect of initial dye concentration (10–40 ppm), (d) influence of radical scavengers (no scavenger, KI, CH₃OH, and NaN₃), (e) effect of solution pH (3–12) and (f) reusability cycles (n = 0–3).

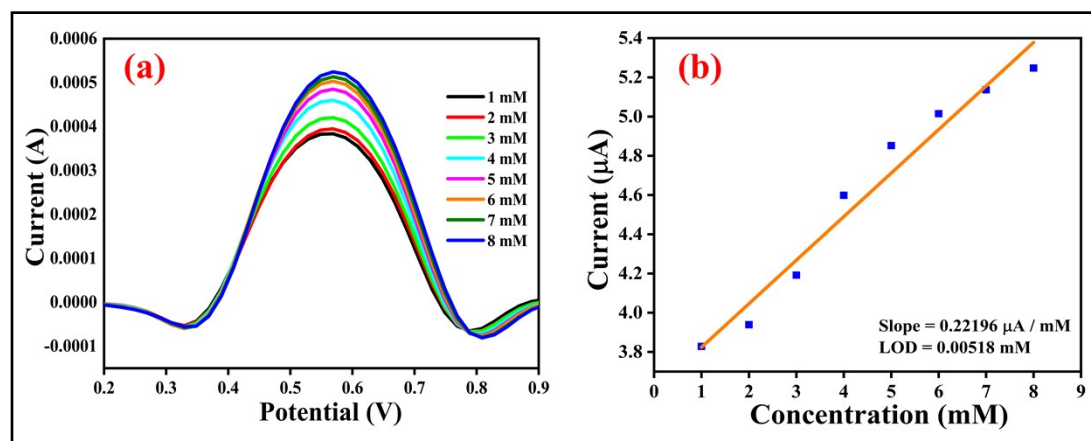


Figure S5. (a) Electrochemical current response of the electrode at different analyte concentrations (1–8 mM). (b) Corresponding calibration plot showing a linear relationship between current and concentration, with a sensitivity of 0.22196 μA mM⁻¹ and a limit of detection (LOD) of 0.00518 mM.